Langmuir Article

pubs.acs.org/Langmuir

Interaction of Surfactants with Hydrophobic Surfaces in Nanopores

Claudiu Brumaru and Maxwell L. Geng*

Department of Chemistry, The Nanoscience and Nanotechnology Institute, Center for Biocatalysis and Bioprocessing and Optical Science and Technology Center, University of Iowa, Iowa City, Iowa 52242, United States

Received August 4, 2010. Revised Manuscript Received October 8, 2010

Surfactant-induced wetting of hydrophobic nanopores is investigated. SDS micelles interact with the C18 layer on the nanopore walls with their hydrophobic tails, creating a charged wall lining with their head groups and inducing a breakthrough of the aqueous solution to wet the pores. The surface coverage of the surfactant molecules is evaluated electrophoretically. A surprising discovery is that pore wetting is achieved with 0.73 μmol/m^2 coverage of SDS surfactant, corresponding to only 18% of a monolayer on the walls of the nanopores. Clearly, the surfactant molecules cannot organize as a compact uninterrupted monolayer. Instead, formation of hemimicelles is thermodynamically favored. Modeling shows that, to be consistent with the experimental observations, the aggregation number of hemimicelles is lower than 25 and the size of hemimicelle is limited to a maximum radius of 11.7 Å. The hydrophobic tails of SDS thus penetrate into and intercalate with the C18 layer. The insight gained in the C18−surfactant interactions is essential in the surfactant-induced solubilization of hydrophobic nanoporous particles. The results have bearing on the understanding of the nature of hydrophobic interactions.

Introduction

Hydrophobic interactions play a pivotal role in the stability of various assemblies organized on the mesoscopic scale in biological structures that reside in aqueous environments.[1,2] Self-assembly of bilayers and vesicles, formation of micelles, and protein folding are just several examples of vital biological processes. The main manifestation of hydrophobic interactions is represented by the tendency of hydrophobic groups or entities to cluster together in an aqueous environment. Extensive studies have suggested that the low solubility of apolar solutes in water is due to both the molecular structure of water and the shape and chemical structure of the solute molecules themselves.[3] The range of the "true" hydrophobic interactions is considered to be < 20 nm.[4] There are attraction forces acting between hydrophobic surfaces for separations much greater than 20 nm, but they are considered to be related to surface preparation techniques rather than to the hydrophobicity of the surfaces.[3]

Nanoporous materials contain networks of interconnected pores with dimensions at nanometer scale. These materials have found widespread applications in chemistry, biology, and medicine. Their properties mimic those of biological channels, nanopores spanning across a lipid bilayer membrane of biological cells.[5] The molecular transport processes such as wetting, diffusion, adsorption, and desorption at nanometer dimensions are different from bulk processes. Molecular dynamic simulations have shown that the diffusion of molecules slows down when the diameter of the nanopores becomes smaller, a size dependence that does not appear at bulk dimensions.[6]

Interaction of aqueous solutions and hydrophobic nanopores has been extensively studied and has shown significant complexity. Cylindrical hydrophobic nanopores cannot be wetted by an aqueous solution when the dimensions of the nanopore are within the range of hydrophobic interactions, as demonstrated in the molecular dynamic simulation carried out by Beckstein et al. However, for a pore with a conical opening, the entry of water molecules is regulated by the geometry of the opening region, the radius of the nanopores, and the extent of hydrophobicity.[5] Liu et al. have also found that the spontaneous water infiltration into hydrophobic nanopores is strongly dependent on their shape. Their molecular dynamic simulation using carbon nanocones as the model structure revealed that conical hydrophobic nanopores allow water infiltration when the apex angle is large. The sharp conical nanopores as well as the perfect cylindrical ones prohibit the access of water inside.[7] Interestingly, Hummer et al. have found, based on their simulation conducted on a nonpolar carbon nanotube (CNT), that hydrophobic channels can have significant water occupancy. Water molecules penetrate the CNT spontaneously and subsequently are transported through it in a pulse-like manner. However, even small perturbations of the polarity of the channel affect its hydration.[8] In addition to simulation studies, a variety of experimental studies have been conducted to investigate wetting of hydrophobic nanopores by aqueous solutions. Confocal imaging experiments using C18-derivatized silica particles with 10 nm nanopores showed that the inner hydrophobic surface of nanopores remained unwetted after 24 h of conditioning with water.[9,10] ^{1}H NMR experiments conducted on porous glass treated with hexamethyldisilazane (HDMS)/*n*-hexane solutions showed that the mobility of H_2O molecules into nanopores was reduced in comparison to untreated glass due to so-called

*Corresponding author. Maxwell L. Geng, lei-geng@uiowa.edu, (319)335-3167.

(1) Lum, K.; Chandler, D.; Weeks, J. D. *J. Phys. Chem. B* **1999**, *103*, 4570.
(2) Chandler, D. *Nature* **2005**, *437*, 640.
(3) Meyer, E. E.; Rosenberg, K. J.; Israelachvili, J. *Proc. Natl. Acad. Sci. U.S.A.* **2006**, *103*, 15739.
(4) Ederth, T.; Liedberg, B. *Langmuir* **2000**, *16*, 2177.
(5) Beckstein, O.; Biggin, P. C.; Sansom, M. S. P. *J. Phys. Chem. B* **2001**, *105*, 12902.
(6) Liu, Y. C.; Wang, Q.; Lu, L. H. *Langmuir* **2004**, *20*, 6921.
(7) Liu, L.; Zhao, J. B.; Yin, C. Y.; Culligan, P. J.; Chen, X. *Phys. Chem. Chem. Phys.* **2009**, *11*, 6520.
(8) Hummer, G.; Rasaiah, J. C.; Noworyta, J. P. *Nature* **2001**, *414*, 188.
(9) Zhong, Z. Ph.D. dissertation, The University of Iowa, 2007.
(10) Skvortsova, Y.; Freeney, R.; Zhong, Z.; Geng, L. *Anal. Chem.* **2010**, *82*, 6712.

"hydrophobic hydration" of water around trimethylsilyl (TMS) groups.[11]

Different approaches have been devised to promote and facilitate the wetting of hydrophobic nanopores. A series of molecular dynamic simulations have shown that water and ion permeation of hydrophobic nanopores embedded in membranes can be regulated by either the electric polarization of the membrane material[12] or the ion concentration gradient across the membrane.[13] In both situations, the water permeation process took place in an intermittent manner and was influenced by pore radius. Although the spontaneous infiltration of a nonwetting liquid like pure water does not occur, the external pressure can be used to force water into hydrophobic nanopores. For instance, for mesoporous silica particles with pore radius in the range 2−4 nm and derivatized with a monolayer of TMS, the necessary external pressure, termed intrusion pressure P_{intr}, ranges within 20−40 MPa. Helmy and co-workers hypothesized that the formation of a wetting vapor-like film, with an average thickness of 0.56 ± 0.09 nm, between the liquid water and the hydrophobic wall is responsible for the failure of the Laplace equation to predict the correct P_{intr} (underestimation of experimental values by 1.5−2-folds).[14] One of the common methods to increase the wettability is to add organic solvents to pure water. The composition threshold of the mixture depends on the nature of the solvent and the nature and coverage density of the hydrophobic ligand of the nanopores and the nanopore radius. Confocal imaging experiments carried out by Freeney et al. determined the exact composition threshold of acetonitrile/water mixture to be 25%/75% (v/v) for wetting C18-derivatized silica particles with 10 nm pores.[15] One other approach is to modify the native surface of nanopore with various functional groups to change the hydrophilicity of the pore surface. For instance, Vlassiouk et al. used a photochromic spiropyran as a light-controlled hydrophobicity switch for nanoporous alumina membrane. Upon exposure to UV light, the hydrophobic compound isomerizes to a more polar form (merocyanine) to allow water penetration.[16]

The interaction of surfactants and solid surfaces at the bulk dimensions has been the subject of extensive studies using techniques such as calorimetry,[17] ellipsometry,[18,19] FTIR,[20] Raman,[21] fluorescence spectroscopy,[22,23] scanning tunneling microscopy (STM),[24] linear and nonlinear optical spectroscopy,[25] neutron reflection,[26] and atomic force microscopy (AFM).[24,27−34] A main goal of the investigation is to elucidate the structure that is formed by surfactant molecules on the surface. Among the surfactants, adsorption of anionic sodium dodecyl sulfate (SDS) on various substrates has been intensely investigated. The surfaces vary from hydrophilic ones such as silica,[25] alumina,[21] and positively charged self-assembled monolayer (SAM) on gold[28,29] to hydrophobic ones such as graphite,[32,34,35] gold,[24] carbon nanotubes,[36] alkyl mercaptan SAM,[28] or undecanethiol SAM[29] on gold, silica derivatized with methyl (C1)[33] or octadecyl (C18) groups.[20,23] Depending on the nature of the substrate and the surfactants, different models have been proposed to describe the mechanism of adsorption. For instance, AFM investigations of Manne et al.[31] using cationic surfactants showed that a negatively charged surface, such as silica at pH 6.3, leads to formation of symmetrical dots suggesting spherical micelles. On the contrary, mica generated meandering stripes of adsorbed surfactants, suggesting cylindrical aggregates flattened at the bottom in order to increase the contact between the headgroups and the surface. Cationic surfactants also formed long stripes on hydrophobic graphite, but they were straight and parallel, suggesting the formation of half-cylindrical aggregates in which the bottom plane of molecule is oriented with tails parallel to a substrate symmetry axis. Another possible model to account for the adsorption of ionic surfactants on hydrophobic substrates prepared by derivatization with long hydrocarbon chains is the formation of a monolayer at concentration around critical micellar concentration (CMC).[28] The model assumes that surfactant molecules form a packed layer with their hydrophobic tails interpenetrating the hydrocarbon chains of the surface and their charged headgroup exposed to solution. Using video microscopy, Wasan investigated the removal of oil droplets from a glass surface with a surfactant solution.[37] The interaction of the micelles with the wedge film surfaces results in an increase in the disjoining pressure that drives the aqueous micellar solution forward to detach the oil drop. These studies were all conducted on large planar substrates. It is of great interest to investigate the structure of surfactant molecules adsorbed on the surface of nanopores.

In this work, we study the adsorption of SDS molecules in hydrophobic nanopores. We have measured the amount of SDS adsorbed on C18-derivatized mesoporous silica particles with a nominal pore diameter of 9 nm. We propose that hemisphere-shaped hemimicelles are the most probable structure attained by SDS molecules on the hydrophobic surface of the nanopores. We conclude that the intercalation of the hydrophobic tails of SDS into the C18 layer is obligatory regardless of the aggregation number of the hemimicelle.

Experimental Section

Chemicals and Materials. Sodium dodecyl sulfate (SDS, ($NaC_{12}H_{25}SO_4$), sodium molibdate monohydrate ($Na_2MoO_4 \cdot H_2O$), and chloroform ($CHCl_3$) were purchased from Fisher Scientific and used as received. Deionized water (18.2 MΩ·cm) was freshly produced daily and degassed by sonication.

(11) Hirama, Y.; Takahashi, T.; Hino, M.; Sato, T. *J. Colloid Interface Sci.* **1996**, *184*, 349.
(12) Allen, R.; Melchionna, S.; Hansen, J. P. *Phys. Rev. Lett.* **2002**, *89*.
(13) Dzubiella, J.; Hansen, J. P. *J. Chem. Phys.* **2005**, *122*.
(14) Helmy, R.; Kazakevich, Y.; Ni, C. Y.; Fadeev, A. Y. *J. Am. Chem. Soc.* **2005**, *127*, 12446.
(15) Freeney, R. Unpublished results, **2009**.
(16) Vlassiouk, I.; Park, C. D.; Vail, S. A.; Gust, D.; Smirnov, S. *Nano Lett.* **2006**, *6*, 1013.
(17) Kiraly, Z.; Findenegg, G. H. *J. Phys. Chem. B* **1998**, *102*, 1203.
(18) Tiberg, F.; Jonsson, B.; Tang, J.; Lindman, B. *Langmuir* **1994**, *10*, 2294.
(19) Tiberg, F.; Jonsson, B.; Lindman, B. *Langmuir* **1994**, *10*, 3714.
(20) Montgomery, M. E.; Wirth, M. J. *Anal. Chem.* **1992**, *64*, 2566.
(21) Somasundaran, P.; Kunjappu, J. T.; Kumar, C. V.; Turro, N. J.; Barton, J. K. *Langmuir* **1989**, *5*, 215.
(22) Levitz, P.; Vandamme, H.; Keravis, D. *J. Phys. Chem.* **1984**, *88*, 2228.
(23) Montgomery, M. E.; Wirth, M. J. *Langmuir* **1994**, *10*, 861.
(24) Burgess, I.; Jeffrey, C. A.; Cai, X.; Szymanski, G.; Galus, Z.; Lipkowski, J. *Langmuir* **1999**, *15*, 2607.
(25) Tyrode, E.; Rutland, M. W.; Bain, C. D. *J. Am. Chem. Soc.* **2008**, *130*, 17434.
(26) Turner, S. F.; Clarke, S. M.; Rennie, A. R.; Thirtle, P. N.; Cooke, D. J.; Li, Z. X.; Thomas, R. K. *Langmuir* **1999**, *15*, 1017.
(27) Carmichael, M.; Vidu, R.; Maksumov, A.; Palazoglu, A.; Stroeve, P. *Langmuir* **2004**, *20*, 11557.
(28) Hu, K.; Bard, A. J. *Langmuir* **1997**, *13*, 5418.
(29) Levchenko, A. A.; Argo, B. P.; Vidu, R.; Talroze, R. V.; Stroeve, P. *Langmuir* **2002**, *18*, 8464.
(30) Manne, S.; Cleveland, J. P.; Gaub, H. E.; Stucky, G. D.; Hansma, P. K. *Langmuir* **1994**, *10*, 4409.
(31) Manne, S.; Gaub, H. E. *Science* **1995**, *270*, 1480.
(32) Paruchuri, V. K.; Nalaskowski, J.; Shah, D. O.; Miller, J. D. *Colloids Surf., A* **2006**, *272*, 157.
(33) Wolgemuth, J. L.; Workman, R. K.; Manne, S. *Langmuir* **2000**, *16*, 3077.
(34) Wanless, E. J.; Ducker, W. A. *J. Phys. Chem.* **1996**, *100*, 3207.
(35) Sammalkorpi, M.; Panagiotopoulos, A. Z.; Haataja, M. *J. Phys. Chem. B* **2008**, *112*, 2915.
(36) Tummala, N. R.; Striolo, A. *ACS Nano* **2009**, *3*, 595.
(37) Wasan, D. T.; Nikolov, A. D. *Nature* **2003**, *423*, 156.

Table 1. Physicochemical Properties of Silica Particles

parameter	10 μm silica 100 Å (Luna) underivatized silica	C18-derivatized silica
particle size (μm)	8.54	
pore diameter (Å)	93	73[a]
surface area (m^2/g)	426	256[a]
pore volume (mL/g)	1.0	0.47[a]
Bonded Phase Analysis of C18-Derivatized Silica		
total carbon (%)	17.84	
surface coverage (μmol/m^2)	3.04	

[a] Calculated values (Supporting Information).

The C18-derivatized silica particles were obtained from Phenomenex (Torrance, CA). The physicochemical properties of the particles are listed in Table 1. Underivatized particles have a diameter of 8.54 μm and an average pore diameter of 93 Å. In the particles under study, the surface is derivatized with a C18 layer.

Methods. *Particle Wetting*. The C18-silica particles were completely solubilized by immersing the particles into the SDS solution followed by consecutive sonication and shaking. The wetted particles were allowed to settle for approximately 48 h to clarify the solution. The particles have sedimented out of the solution and formed a dense layer at the bottom of the sample vial, as shown in the image of the four samples in Figure I.1 of the Supporting Information. Aliquots of the clarified solution above the particle layer were collected and diluted to a concentration that falls within the concentration range of the calibration curve for electrophoretic analysis. Because of the clear separation of the particles and the supernatant solution, no additional preparation steps, such as filtration or centrifugation, were necessary.

Capillary Electrophoresis. SDS quantification was carried out using a Beckman P/ACE MDQ (Beckman Coulter, Fullerton, CA) capillary electrophoresis system. Polyimide-coated fused silica capillaries (Polymicro Technologies, Phoenix, AZ) were used in the separations. Prior to use, the capillaries were preconditioned consecutively with 0.1 M sodium hydroxide, 0.1 M hydrochloric acid, deionized water, and run buffer. The temperature of the capillaries was maintained at 25 °C. The working parameters were as follows: buffer 5 mM sodium molibdate; UV−visible detection at 214 nm; capillary, total length = 31.0 cm, effective length = 20.5 cm; 75 μm I.D.; run voltage +25 kV; pressure injection at 0.5 psi for 7 s.

Results and Discussion

Measurement of SDS Surface Concentration in Nanopores. The amount of SDS adsorbed on the surface of C18-derivatized silica particles was measured by quantifying the concentrations of free SDS in the original solution and then after sample processing/particle solubilization. We applied the CE procedure used by Bächmann et al.[38] to measure the SDS level in an aqueous suspension of nonporous Chromspher RP-18 1.5 μm particles. The method determines the concentration of SDS as monomers in solution using calibration curves built in the submicellar range 0−2.5 mM (micelles start to form above CMC of 8.3 mM for SDS[23]). SDS is detected by indirect UV−vis absorption; when molibdate is displaced by SDS molecules in the run buffer of CE, the absorbance of the solution decreased. SDS thus shows a negative peak in the electropherogram. A CE-based method was chosen over the classic Epton method[39] to eliminate the use of toxic organic solvent (chloroform)

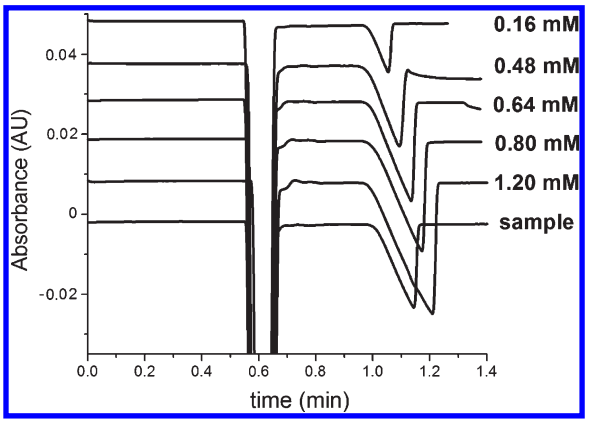

Figure 1. CE analysis of SDS. From top to bottom, electropherograms of calibration standards ranging from 0.16 mM to 1.20 mM and a sample. The electropherograms were displaced for clarity of presentation.

Table 2. SDS Coverage of the Nanopore Surface[a]

sample number	initial SDS concentration (mM)	final SDS concentration (mM)	coverage (μmol/m^2)
1	74.9	51.1	0.69 ± 0.06
2	74.9	48.3	0.78 ± 0.06
3	74.9	50.4	0.71 ± 0.06
4	74.9	49.9	0.73 ± 0.06
	average		0.73 ± 0.03

[a] The error (1 standard deviation) in the coverage for each sample was evaluated from the calibration curve and propagated through the dilution factor. The final error in the average coverage was calculated through error propagation from the samples.

and to enable automation. Typical electropherograms of SDS calibration standard solutions and a sample are presented in Figure 1. The negative SDS peak appears at the migration time of 1 min. The SDS calibration curve was constructed from the integrated peak areas. The correlation coefficients r^2 for several calibration curves were all above 0.99. The uncertainties in sample SDS concentrations were in the range 1−2% from calibration. The surface coverage of SDS was calculated from the amount of SDS molecules that had been adsorbed into the nanopores and the pore area computed from the mass of the particles. The uncertainties in the surface coverage by SDS were evaluated from the calibration and all sampling steps and are listed for every sample in Table 2, as well as the standard deviation of the mean for the average coverage.

SDS Adsorption on Hydrophobic Surface. The adsorption of ionic surfactants on hydrophobic surfaces has been intensively studied. Directed at understanding the interaction between surfactants and surfaces, experiments have been conducted on open (nonconfined), flat, hydrophobic surfaces that are exposed to surfactant solutions at atmospheric pressure.[20,23,24,28,29,32−36] In the other research direction intended to use surfactants as mobile phase additives to improve chemical separations, mesoporous silica particles derivatized with hydrocarbon groups are tightly packed into columns in a typical HPLC configuration. The surfactant solution is forced (pumped) continuously through the column under high pressure, and the amount of surfactant adsorbed is estimated by the change in the concentration of the surfactant in the mobile phase.[40−47] Unlike these studies, the

(38) Bachmann, K.; Gottlicher, B.; Haag, I.; Han, K. Y.; Hensel, W.; Mainka, A. *J Chromatogr., A* **1994**, *688*, 283.
(39) Weatherburn, A. S. *J. Am. Oil Chem. Soc.* **1951**, *28*, 233.
(40) Berthod, A.; Girard, I.; Gonnet, C. *Anal. Chem.* **1986**, *58*, 1356.
(41) Hung, C. T.; Taylor, R. B. *J. Chromatogr.* **1981**, *209*, 175.
(42) Knox, J. H.; Hartwick, R. A. *J. Chromatogr.* **1981**, *204*, 3.
(43) Berthod, A.; Girard, I.; Gonnet, C. *Anal. Chem.* **1986**, *58*, 1359.
(44) Berthod, A.; Girard, I.; Gonnet, C. *Anal. Chem.* **1986**, *58*, 1362.

objective of our work is to understand surfactant-induced wetting of hydrophobic nanopores. Specifically, we investigate the process of SDS adsorption on the inner surface of highly hydrophobic nanopores of C18-derivatized silica particles at atmospheric pressure. The wetting of hydrophobic nanopores is of significant technical interest, not only due to their nanotechnology applications, but also due to their relevance in biological nanopores and channels. There is, however, limited understanding of the wetting process. It is known that an aqueous solution is not able to wet the nanopores of silica particles derivatized with hydrophobic ligands at atmospheric pressure. By applying pressures higher than 17 MPa (limit value known as infiltration pressure), water molecules can be forced to enter the nanopores.[48,49] Since they can interact with both pore surface and water molecules, surfactants lower the infiltration pressure and therefore act as promoter of the wetting process. Yet, the efficiency of this process is both concentration[48,50,51] and pore-size dependent,[52] and surfactants do not lower the infiltration pressure down to the atmospheric pressure. The preparation method that we established enables the wetting of the nanopores *at ambient pressure*.

To elucidate the structure formed by SDS and the C18 hydrophobic surface, we evaluated the average amount of SDS adsorbed on the sedimented particles with the CE method. The level of SDS adsorbed on the pore surface was $0.73 \pm 0.03\ \mu mol/m^2$, corresponding to only 18% of monolayer coverage by SDS in the nanopores. Table 2 shows the coverage of the nanopore surface by SDS molecules for four separate samples. In the sedimented particles, it is expected that the nanopores of the particles are wetted. The fact that complete nanopore wetting was induced with such low surface coverage (18%) of the surfactant was quite surprising and intriguing. A survey of the literature studies of surfactant−hydrophobic surface interactions shows that our observed coverage is quite low. For instance, in studies conducted by pressure pumping SDS solutions through columns packed with similar types of particles the surface coverage increased until the CMC was reached, after which a plateau around $4-5\ \mu mol/m^2$ was observed for micelle concentrations higher than CMC.[40,41,44] Experiments using other types of surfactants with similar lengths of hydrocarbon tails led to surface coverage in the same range.[40,41,44,45] For C18-derivatized silica particles, coverage of $1.8\ \mu mol/m^2$ was found with 3% 1-propanol in solution.[53] Similarly, coverage of $1\ \mu mol/m^2$ was observed using 285 mM SDS aqueous solution.[54] It is noted that the solution was pumped through the column in these experiments, and thus, the pore wetting was influenced by the high pressure. In the investigations conducted on flat hydrophobic surfaces at atmospheric pressure, a range of values have been measured by various authors. A maximum plateau around $4\ \mu mol/m^2$ was recorded for SDS adsorption on undecanethiolate self-assembled monolayer on gold.[29] With C18-derivatized silica plates, an anomalous shape of SDS adsorption isotherm was observed, with a $5.9\ \mu mol/m^2$ peak around CMC (7 mM) followed by a sudden decrease and a plateau at $1.2\ \mu mol/m^2$ starting at 12 mM of SDS.[23] It should be emphasized that these studies were conducted on flat hydrophobic surfaces in direct contact with the solution. In contrast, our study is conducted on hydrophobic nanopores. The interaction between the surfactant molecules and the hydrophobic wall surface of the nanopores effectively decreases the hydrophobicity of surface to make nanopores thermodynamically favorable to the aqueous surfactant solution and thus induces wetting.

In order to elucidate the structure formed by SDS molecules adsorbed on the hydrophobic surface of the nanopores, we validated the surprisingly low SDS surface coverage with multiple replicate experiments. As shown in Table 2, there is excellent consistency in the level of incorporation of SDS into the nanopores for four separate samples. In the calculation, the concentration of SDS inside the nanopores was taken as identical to that of the bulk solution, since thermodynamic equilibrium has been reached over 48 h of sample settlement. The equilibrium was verified spectroscopically by the spectrum of the solution remaining unchanged after equilibrium was reached.[55] The recoveries for several SDS test solutions, covering a wide range of concentrations (8−80 mM) and undergoing the same wetting procedure as the samples with particles, were measured, and all showed values higher than 96%. The overall performance of SDS quantification (calibration linearity, calibration uncertainty) fell in the expected range of values for CE separations.

Particle Density Simulation. That a low surface coverage of the surfactants corresponding to 18% monolayer formation induced nanopore wetting was a surprising observation. We were intrigued to understand how SDS molecules interact with the C18 hydrophobic layer and what structure they form on the surface to facilitate nanopore wetting. Since the wetting process is initiated and supported by the surfactant molecules that interact with hydrophobic C18 ligands, the volume of solution that enters the nanopores is determined by the amount of adsorbed SDS. Only the fraction of the pores where the wall surface is rendered hydrophilic by SDS adsorption is filled with the solution. Naturally, the adsorption process starts from the opening of the pores and gradually progresses inside. There are two possible ways for SDS molecules to cover the pore wall: formation of a compact uninterrupted monolayer or adsorption of dispersed molecules spread on the wall. For the same number of surfactant molecules, the first alternative leads to a lower surface area covered and consequently to less solution wetting of the nanopores than the second possibility. We decided to use the density of the wetted particles as the indicator of how much solution advances into the pores and thus elucidate the mode of SDS-surface interaction.

We carried out the density simulation by considering the three possible components that occupy the nanopores: the solution, SDS adsorbed on the inner wall of the nanopores, and air. We neglected the amount of SDS adsorbed on the outer surface of particles; this surface area is negligible compared to the nanopore surface. In order to evaluate the volume occupied by and the mass of each of the three components, we first calculated the average values of pore volume, pore radius, and pore surface of the silica particles after derivatization with a C18 layer: $V_{pore} = 0.47$ mL/g particles, $R_{pore} = 36.5$ Å, and $A_{pore} = 256\ m^2/g$ particles (see Supporting Information for details). The density of C18-derivatized particles (silica + C18) was $\rho_{solid} = 1.538$ g/mL (see Supporting

(45) Deelder, R. S.; Linssen, H. A. J.; Konijnendijk, A. P.; Vandevenne, J. L. M. *J. Chromatogr.* **1979**, *185*, 241.
(46) Borgerding, M. F.; Hinze, W. L. *Anal. Chem.* **1985**, *57*, 2183.
(47) Gritti, F.; Guiochon, G. *J. Chromatogr., A* **2006**, *1115*, 142.
(48) Punyamurtula, V. K.; Qiao, Y. *Mater. Lett.* **2008**, *62*, 2928.
(49) Surani, F. B.; Han, A.; Qiao, Y. *Appl. Phys. Lett.* **2006**, *89*.
(50) Surani, F. B.; Kong, X. G.; Qiao, Y. *Appl. Phys. Lett.* **2005**, *87*.
(51) Punyamurtula, V. K.; Qiao, Y. *Microporous Mesoporous Mater.* **2007**, *103*, 35.
(52) Han, A. J.; Qiao, Y. *J. Am. Chem. Soc.* **2006**, *128*, 10348.
(53) Dorsey, J. G.; Khaledi, M. G.; Landy, J. S.; Lin, J. L. *J. Chromatogr.* **1984**, *316*, 183.
(54) Borgerding, M. F.; Hinze, W. L.; Stafford, L. D.; Fulp, G. W.; Hamlin, W. C. *Anal. Chem.* **1989**, *61*, 1353.
(55) Skvortsova, Y.; Geng, L. Unpublished results, **2009**.

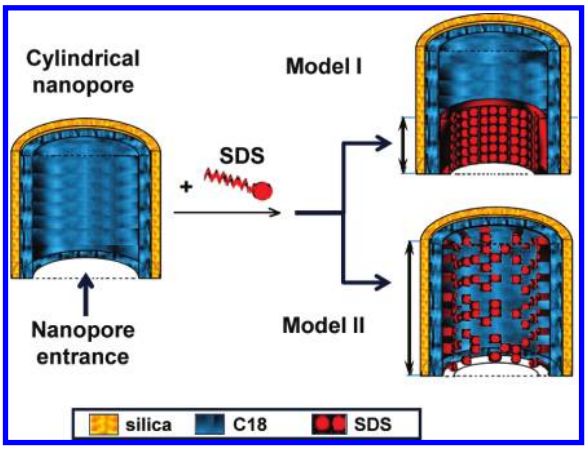

Figure 2. Two models of SDS adsorption with SDS hydrophobic tails oriented away from the surface. Model I: SDS molecules form a compact uninterrupted monolayer on surface; Model II: SDS molecules adsorb to dispersed sites covering a wider area. The maximum level of solution inside the nanopore is marked with up−down arrows.

Information for calculation). Finally, the density is estimated (Supporting Information)

$$\rho_{\text{total}} = \frac{m_{\text{solid}} + \rho_{\text{solution}} V_{\text{solution}} + n_{\text{SDS adsorbed}} \text{MW}_{\text{SDS}}}{\frac{m_{\text{solid}}}{\rho_{\text{solid}}} + V_{\text{pores}}} \quad (1)$$

where m, V, ρ, n, and MW denote mass (g), volume (mL), density (g/mL), number of moles, and molar mass (g/mol) respectively.

The dry particles have a density of 0.89 g/mL and float on the surface of the aqueous solution at the air−solution interface. The SDS-wetted particles, after 48 h of settlement, sedimented out of the solution to form a compact, white layer at the bottom of the sample vial, as shown in Figure I.1 in the Supporting Information. This experimental observation clearly suggests that the wetted particles have a density larger than that of the solution. The filling of the nanopores by the aqueous solution increased the overall particle density and lead to particle sedimentation.

Interaction between SDS Surfactants and the C18 Hydrophobic Surface. *Surfactant Adsorbed As a Compact Layer* (*Model I*). The first model we tested for consistency with our experimental surface coverage was the formation of a dense, uninterrupted, compact monolayer of SDS that covers a fraction of the wall surface starting from the opening of the nanopores. In this structure, the hydrophobic tails of the SDS orient away from the C18 surface. The compact monolayer model is consistent with and properly accounts for literature results that recorded coverage in the range 4−5 μmol/m^2 for particles similar to ours. For a charge density of 40 Å^2/molecule,[38] 4.2 μmol/m^2 corresponds to a compact monolayer of SDS completely covering the C18 layer on the nanoporous surface. The graphical representation of this model, denoted by Model I, is presented in Figure 2. The density of solution can act as an indicator of the particle density. A quick inspection of the density plot for this model (Figure 3A) reveals that only the particles with coverage higher than 22% (corresponding to 0.92 μmol/m^2) become heavier than the solution (density of 0.9982 g/mL at 20 °C[56]) and start to sediment. For the experimental value of SDS coverage of 0.73 μmol/m^2 (corresponding to 18% surface coverage), particles should be floating on the surface of solution, contrary to the experimental observation. As a result, Model I cannot explain how particles (density in dry state of 0.89 g/mL) with 18% of the pore surface covered with surfactants can reach a density higher than 0.9982 g/mL. We need to add a comment regarding the sinking threshold of 0.92 μmol/m^2 (22% coverage). In the evaluation of this threshold, the compact SDS monolayer was set to 11 Å in thickness for density simulation, the smallest of all experimental values in literature observations. For example, the thickness of the SDS layer was determined to be 1.11 ± 0.05 nm on a hydrophobic SAM,[29] 1.36−1.53 nm on gold,[57] and 1.5 ± 0.2 nm on polystyrene.[26] On graphite, SDS formed stripes that were 1.7 ± 0.5 nm thick as measured by AFM.[34] For thicker adsorbed SDS layers, the sinking threshold of particles would become even higher than 0.92 μmol/m^2, and consequently, the inability of Model I to explain the experimental observation would be more significant.

Surfactant Adsorbed As Individual Dispersed Molecules (*Model II*). The second possibility of SDS−surface interaction is that SDS molecules are dispersed on the nanopore surface. This interaction can take place with SDS either as individual molecules or as small groups (aggregates) and leads to a wider surface area occupied by the adsorbed SDS. We first considered the model of dispersed individual SDS molecules, denoted by Model II (Figure 2). In this model, the SDS molecules spread out on the surface, with substantial space between them. The pore surface that is modified by SDS surfactants is thus much larger than or expanded from the surface that a compact, uninterrupted SDS layer would cover. The factor of expansion is defined as the dispersion factor f^*. In this model, the hydrophobic tails of the surfactant molecules interact directly with the C18 layer, while the negatively charged head groups are extended into the pore volume, creating dispersed hydrophilic centers on the hydrophobic wall surface of the nanopores. When the density of the charged head groups on the surface is sufficiently high, the existence of an aqueous phase in the nanopore is thermodynamically favored, leading to wetting. Any pore volume enclosed by SDS-modified surface is wetted by water; this SDS−surface structure thus allows for a larger volume of solution to enter the nanopores. The dispersion factor f^* reflects the decrease in charge density and is determined as the ratio of the area covered by SDS in a specific surface structure to the area of surface covered by the same amount of SDS in a compact monolayer structure. The monolayer represents the minimum area covered and corresponds to a charge density of 40 Å^2/molecule and no dispersion ($f^* = 1$).

Figure 3B,C shows the particle density as a function of the SDS coverage and the dispersion factor f^* (see Supporting Information for detailed calculation). The particle density increases with the dispersion factor in Model II. As the result of spreading of adsorbed SDS molecules on the pore surface, Model II (Figure 3C) could explain the particle behavior for any dispersion factor $f^* > 1.3$ that leads to a particle density greater than that of the solution. However, another important piece of information was offered by a set of confocal imaging experiments conducted in our lab[55] that showed that the sedimented particles were completely filled with solution. Briefly, Rhodamine 6G, a fluorescent probe with excellent water solubility (500 mg/L at 25 °C[58]) was used as a tracer for visualizing the solution penetration into nanopores. The images revealed that the particles were completely filled (fluorophore present in the entire particle). To account for these results, the maximum dispersion factor, f^* 5.6, is required in Model II in order for SDS molecules to cover the entire nanopore

(56) *CRC Handbook of Chemistry and Physics*, 89th ed.; Lide, D. R., Ed., 2008−2009.

(57) Burgess, I.; Zamlynny, V.; Szymanski, G.; Lipkowski, J.; Majewski, J.; Smith, G.; Satija, S.; Ivkov, R. *Langmuir* **2001**, *17*, 3355.

(58) Cheruvu, N. P. S.; Kompella, U. B. *Invest. Ophthalmol. Vis. Sci.* **2006**, *47*, 4513.

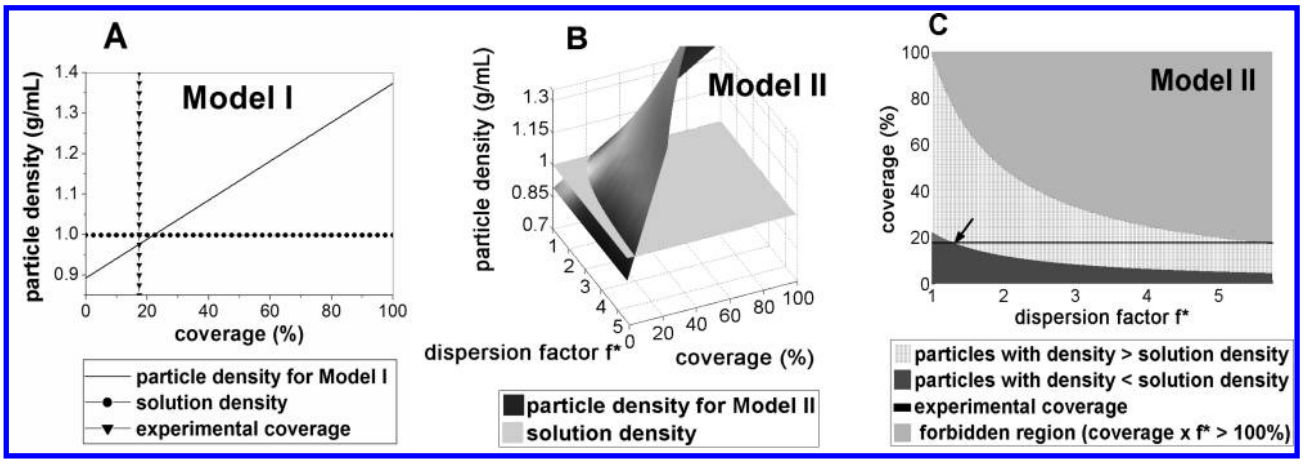

Figure 3. Particle density as a function of the amount of adsorbed SDS and the dispersion factor. SDS adsorbed is expressed as surface coverage (%). 100% coverage corresponds to 4.2 μmol/m^2 of SDS. The dispersion factor is 1 for Model I. The forbidden region in (C) corresponds to an effective coverage larger than 100%, which is physically impossible. The arrow indicates the dispersion factor (1.3) where the particle density reaches that of the solution and the particles start to sediment.

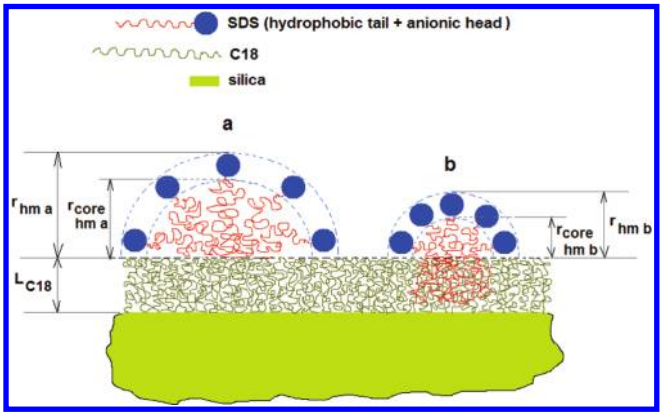

Figure 4. Half-sphere-shaped SDS hemimicelles adsorbed on C18-derivatized silica. Hemimicelle a: the entire length of SDS tail (12 C atoms) participate in the formation of the hydrophobic core. Hemimicelle b: a fraction of the SDS tail intercalates into the C18 layer. Both hemimicelles have the same aggregation number. L_{C18} represents the average thickness of C18 layer, $r_{core\ hm}$ is the radius of the hydrophobic core of the hemimicelle, and r_{hm} is the radius of the hemimicelle.

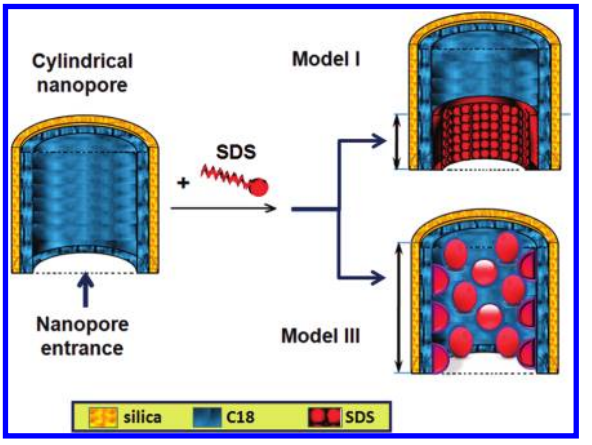

Figure 5. SDS forming hemimicelles on the hydrophobic surface of nanopores (Model III). The size of hemimicelles depends on the aggregation number and the degree of intercalation of the SDS tails into the C18 layer.

surface and thus for the solution to completely fill the nanopores (the cross point between the experimental coverage and the boundary between particle density and forbidden region in Figure 3C). The dispersion brings the charge density to around 224 Å^2 per molecule. This condition mandates that SDS interact with the C18 layer as isolated molecules with an average intermolecular distance of 15 Å. Model II forces the hydrophobic tails of SDS to have a large contact area with water molecules, which is unfavorable thermodynamically.

Hemimicelle Formation (*Model III*). The next possible structure, Model III, is the formation of hemimicelles, or hemispherical aggregates of surfactants. This structure is favored on some flat hydrophobic surfaces, as observed by AFM studies. Investigations conducted on hydrophobically modified silica and graphite surfaces[30,31,33] have shown that silica as a substrate leads to circular aggregates, while the high structural symmetry of graphite leads to parallel stripes of adsorbed surfactants on this surface. Consequently, in density simulation we used the hemispherical shape to model a hemimicelle formed on the nanopore surface of the C18-silica particles. The hydrophobic tails of SDS are allowed to intercalate into the C18 layer (Figure 4). This was also suggested by Montgomery and Wirth in their studies on silica substrates.[23] In addition, Fadeev and McCarthy[59] showed that alkane liquids penetrate into alkyldimethylsilane monolayers covalently grafted to silica. The graphical representation of SDS adsorption into nanopores in Model III is presented in Figure 5.

We used the following assumptions and parameters for the density simulation in Model III (Supporting Information for details): (1) A hemimicelle consists of a hydrophobic core and a charged shell. (2) The radius and volume of the hydrophobic core are calculated using the Tanford formulas;[60] the volume of one SDS tail was thus set to 350 Å^3. (3) The diameter of the ionic headgroup of SDS was set to 4.8 Å (estimated based on Bruce et al.).[61]

In our simulation, the hemimicelle aggregation number was scanned from 2 to 31 (the aggregation number for a full spherical micelle in SDS bulk solution is 62[60]) and the degree of penetration

(59) Fadeev, A. Y.; McCarthy, T. J. *Langmuir* **1999**, *15*, 3759.
(60) Tanford, C. *J. Phys. Chem.* **1972**, *76*, 3020.
(61) Bruce, C. D.; Berkowitz, M. L.; Perera, L.; Forbes, M. D. E. *J. Phys. Chem. B* **2002**, *106*, 3788.

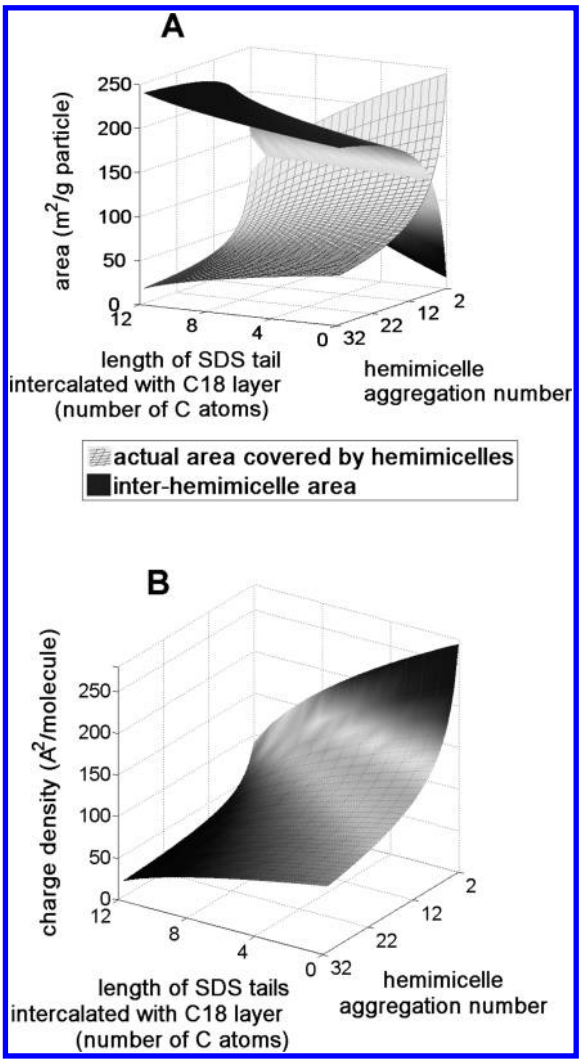

Figure 6. Actual pore surface area covered by hemimicelles (A) and charge density (B) as a function of the aggregation number and the length of SDS tails that intercalate into the C18 layer. Experimental SDS adsorbed = 0.73 μmol/m^2. The total pore area is 256 m^2/g.

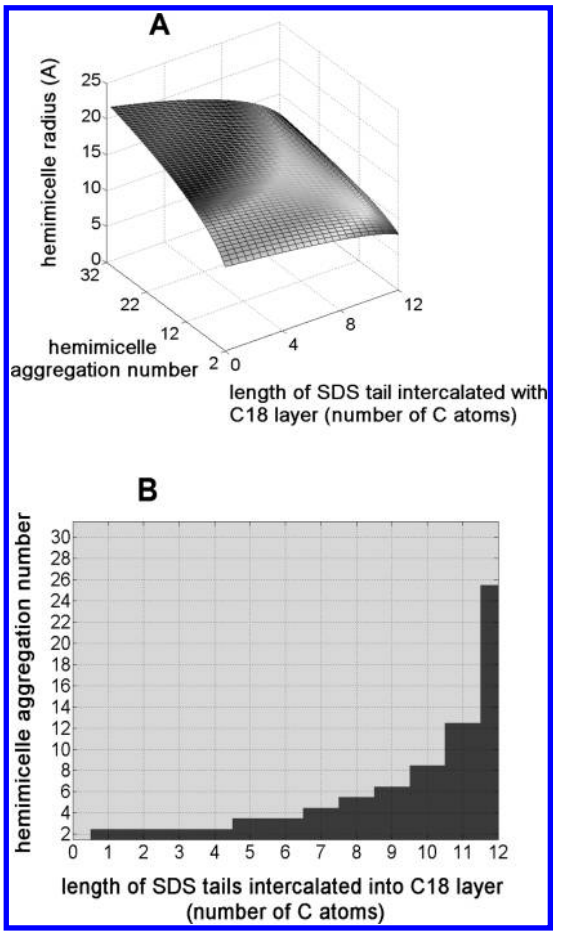

Figure 7. Hemimicelle radius (A) as a function of the aggregation number and length of SDS tails that intercalate into the C18 layer. (B) shows the region corresponding to hemimicelle radii of < 11.7 Å (dark area).

of SDS tails into the C18 layer, expressed in number of C atoms, was scanned from 0 to 12 to explore the entire sample space.

Figure 6 shows surface coverage of the hemimicelles (Figure 6A) and charge density (Figure 6B) as a function of the aggregation number and the length of SDS tails that penetrate into the C18 layer. The overall thermodynamics of the system is decided by two driving forces. First, SDS hemimicelles tend to achieve the optimum charge density of 75 Å^2/molecule, the charge density of bulk SDS micelles. This charge density is regulated by two opposite tendencies: the hydrophobic core favors a high charge density on the surface of hemimicelle in order to be protected against direct contact with water; the negatively charged sulfate groups will exert electrostatic repulsions in case of high charge density. Second, C18 chains covering the nanopore surface favor a low interhemimicelle area in order to minimize their direct contact with water. The plots in Figure 6 show the overall effect of these thermodynamic forces.

There exists a large number of possible combinations of hemimicelle aggregation number and length of SDS intercalated into the C18 layer. The number of combinations is reduced by the steric constraint that, after SDS adsorption, there should be sufficient space available in the pore for intact SDS micelles in solution to enter the nanopores. This limitation is supported by a set of preliminary experiments conducted in our lab[55] confirming that full SDS micelles were able to enter the nanopores. We used ratiometric multiphoton-excitation confocal imaging to study the wetting of similar particles by SDS solutions. The solvatochromic fluorophore PRODAN (6-propionyl-2-dimethylaminonaphthalene) is sensitive to the polarity of its environment and thus revealed the presence of SDS micelles in wetted nanopores. The diameter of an SDS micelle with an aggregation number 62 is 44 Å calculated with the Tanford formula.[60] Taking into account the diameter of C18-derivatized pores in our particles, 73 Å (see Supporting Information), and assuming that a full micelle would need a water layer of at least one molecule thickness (2.8 Å[61]) between its ionic head groups and those of adsorbed SDS to be able to travel freely through the nanopore, the hemimicelle radius cannot be larger than 11.7 Å (44 Å micelle diameter +2 × 2.8 Å water layer +2 × 11.7 Å hemimicelle on C18 = 73 Å). Figure 7 shows the dependence of hemimicelle radius on its aggregation number and the length of SDS tails that intercalate into the C18 layer (Figure 7A). The 2D plot in Figure 7B shows the region corresponding to hemimicelle radii of < 11.7 Å.

Results of the Model with Hemimicelles. Examining Figure 7B, we extract two significant observations: first, the hemimicelle aggregation number has to be ≤25 (the maximum aggregation number that falls within the gray region); second, SDS tails have to intercalate partially or totally into the C18 layer regardless of the aggregation number. Considering that the aggregation

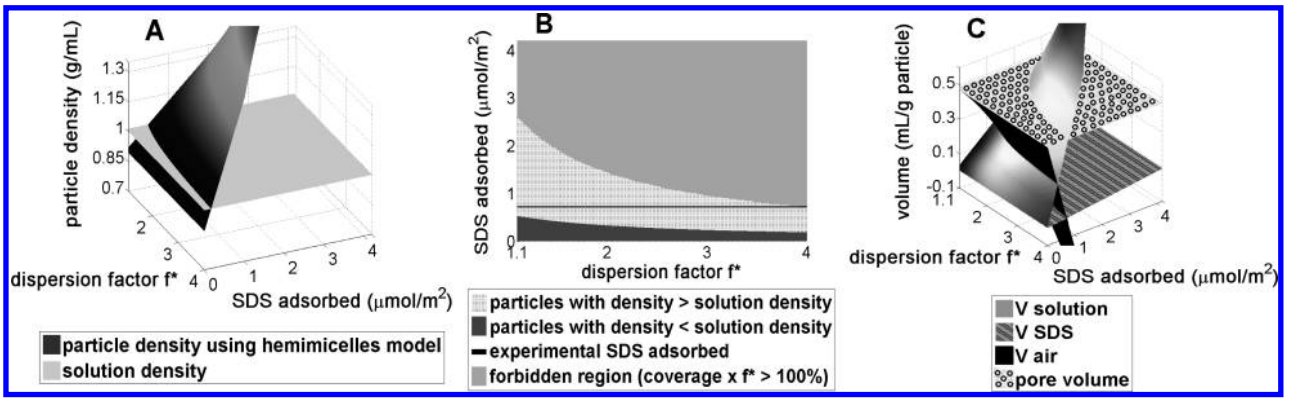

Figure 8. Particle density (A and B) and volumes of components inside of nanopore (C) as a function of the amount of SDS adsorbed and dispersion factor *f** for adsorbed hemimicelles with aggregation number 7 and ten C atoms of the SDS tails intercalating into the C18 layer. The region in C for which the volume of solution becomes higher than the pore volume (0.47 mL) corresponds to forbidden region in B.

numbers 2 and 3 seem improbable for hemimicelle formation and they have not been observed experimentally, the hydrophobic tails have to use at least half of their length to intercalate into the C18 layer. On the basis of steric consideration in Figure 7B and the charge density in Figure 6B, the most thermodynamically favored hemimicelles (with charge density ~75 Å^2/molecule) that are also smaller than 11.7 Å in radius should have aggregation numbers in the range 4−8.

Gu and Rupprecht[62] have theoretically calculated a value of 7 for globular SDS hemimicelles. Assuming an aggregation number 7 for our case, the minimum number of C atoms to be buried into C18 layer has to be 10. For this specific case, the hemimicelle radius is 11.3 Å, with a core radius of 6.5 Å, a charge density of 70.7 Å^2/molecule, and an actual (effective) occupied area of 64.2 m^2/g particle. Figure 8 shows the simulated particle density as a function of SDS coverage and dispersion factor *f** (Figure 8A,B), as well as the volumes of components (air, solution, and adsorbed SDS) inside the nanopores (Figure 8C) for hemimicelles with aggregation number 7 and 10 C atoms of the SDS tails intercalating into the C18 layer. This leaves an average of two C atoms of each SDS chain to extend into the nanopore volume to form the hemimicelle. It is expected that some of the SDS molecules could have their hydrophobic tails completely buried in the C18 layer while others have larger fractions of their tails extended into the nanopore to form the hemispherical aggregates. Note that the smallest dispersion factor is 1.10, for the hexagonal close-packing of the hemimicelles. For nanopores completely filled with solution (our experimental observation), the actual covered area is 64.2 m^2/g particles, intermicellar area is 191.8 m^2/g particle, the total covered area is 256 m^2/g particles, and the dispersion factor is 4.0 (256/64.2).

We will highlight a couple of details of the proposed Model III. First, we assumed that the nanopores of sedimented particles were completely filled with solution. The confocal imaging experiments confirmed this assumption, but there is still the possibility for some particles to have a small fraction of pores filled with air (nonwetted) impossible to detect due to the inherent resolution limit of the optical microscopy. Indeed, confocal fluorescence imaging has shown heterogeneity of physicochemical properties of these nanoporous particles that potentially resulted from the pore size distribution.[63,64] Second, we performed the simulation using the average pore size of 73 Å. Undoubtedly, a pore size distribution exists so that the actual access of SDS micelles from bulk solution could be restricted for narrower nanopores. Consequently, it is possible that, for this population of nanopores, SDS molecules organize in smaller hemimicelles. However, the limitation of a maximum radius of 11.7 Å restricts the aggregation numbers to the low range of 4−8. On the other hand, in the wider pores the spatial restriction is relaxed and the SDS surfactant molecules can form larger hemimicelles by not having to insert a significant fraction of their hydrocarbon chains into the C18 layer. This would lead to a larger effective area of the hydrophobic surface covered by the charged surface of the hemimicelles, promoting pore wetting by aqueous solutions. Overall, the formation of hemimicelles, Model III, leads to a more thermodynamically stable system compared to the adsorption of dispersed individual molecules, Model II. The adsorption of SDS molecules as a compact layer, Model I, cannot explain the sedimentation of the wetted particles for the experimental coverage of 0.73 μmol/m^2.

We are planning to vary the bulk SDS concentration in order to investigate its influence on the surface coverage by using the developed particle preparation protocol at atmospheric pressure. Preliminary tests conducted at a lower SDS concentration of 60 mM showed efficient pore wetting and lead to SDS adsorption of ~0.51 μmol/m^2, corresponding to only 12.1% of a monolayer coverage. This even lower surface coverage mandates a larger dispersion factor.

The simulation above assumes that the entire pore volume enclosed by the SDS-modified surface is wetted and occupied by the aqueous solution. This condition is valid for the hydrophilic surface lined by the head groups of SDS surfactants. The C18 surface that is not directly covered by SDS remains hydrophobic and water behaves as a nonwetting solution for this fraction of the pore wall. It is known that a low-density fluid or vapor layer is formed between the hydrophobic surface and the nonwetting aqueous solution when they are brought into contact.[1] The formation of this vapor layer reduces the pore volume available for the surfactant solution. The overall effect is a decrease in the net density of the particles. Helmy measured the thickness of the vapor layer in a similar system, mesoporous silicas with 2−4 nm pores and a hydrophobic pore surface generated with a trimethylsilyl monolayer.[14] The average thickness was 0.56 nm with a range of 0.42−0.64 nm.

We examined the influence of this vapor layer on the structural understanding from our experiments and simulation, using the average thickness presented by Helmy. Model I, the formation of a compact noninterrupted SDS layer, is not affected, since the entire SDS-modified surface has become hydrophilic and the

(62) Gu, T.; Rupprecht, H. *Colloid Polym. Sci.* **1990**, *268*, 1148.
(63) Lowry, M.; He, Y.; Geng, L. *Anal. Chem.* **2002**, *74*, 1811.
(64) Zhong, Z. M.; Lowry, M.; Wang, G. F.; Geng, L. *Anal. Chem.* **2005**, *77*, 2303.

aqueous solution is energetically stable over the surface. Model II has SDS surfactants dispersed on the surface as individual molecules. This model is the least stable among the three thermodynamically and will not be discussed further. In Model III, the space between SDS hemimicelles remains hydrophobic and requires a wetting fluid—the vapor layer, on top of the C18. We repeated the simulation by introducing a 0.56 nm vapor layer on the inter-hemimicelle surface. This vapor layer occupies a fraction of the pore volume that the aqueous solution is excluded from, reducing $V_{solution}$ in eq 1 and thus the overall density of the particle. In Table 4.1 of the Supporting Information, we show examples of the particle density for two types of hemimicelles that are allowed by the geometrical restriction: aggregation numbers of 4 and 7, with 7 and 10 C-atoms of the hydrophobic tail buried in the C18 layer, respectively. The vapor layer leads to 17% and 24% reduction in the solution volume, but only changes the overall density of the particles by 5% and 7%, respectively. The lowered density, however, still stays above the solution density for the experimental SDS coverage of 0.73 μmol/m^2 along the entire range of the dispersion factor f^*. The conclusions on SDS-C18 interaction remain unchanged with or without the vapor layer considered. It is noted that the thickness of the vapor layer depends on the architecture of the pores, and accurate calculation for our system will require the measurements of the thickness for silica particles used in our experiments. The density of wetted, solution-filled particles is such that, for sterically allowed hemimicelles, it is expected that the particles are heavy enough to sediment out of the solution, consistent with experimental observations.

Conclusions

The goal of this study was to investigate surfactant-induced wetting of highly hydrophobic nanopores at atmospheric pressure. With our experimental protocols, the nanopores are completely wetted by 80 mM SDS solutions without the need of high pressure pumping. The average amount of adsorbed SDS was 0.73 μmol/m^2, which represents 18% of a compact monolayer on the nanopore surface. The study of nanopore wetting can be viewed and understood in the same way as capillary evaporation. These opposite processes are governed by the same thermodynamic forces and they can take place for surfaces interlaced with hydrophilic and hydrophobic patches. Moreover, they depend on the size and density of the hydrophobic domains. In terms of the actual structure adopted by adsorbed SDS, we demonstrated that surfactant molecules could not organize as a compact, uninterrupted monolayer. Instead, hemimicelles are thermodynamically favored and successfully account for the experimental results. In this model, SDS molecules form hemimicelles on the hydrophobic nanopore surface, lining the pore wall with charged head groups to induce the penetration of aqueous solution and thus wetting of the hydrophobic nanopores. The aggregation number of the hemimicelles cannot exceed 25 and their size is limited to a maximum radius of 11.7 Å. Regardless of the aggregation number, a fraction of the SDS hydrophobic tail has to penetrate and intercalate into the C18 layer.

Acknowledgment. The support by the National Science Foundation (Grant 0911691) and the University of Iowa (MPSFP) is gratefully acknowledged. We thank the Center for Biocatalysis and Bioprocessing of the University of Iowa for a graduate fellowship to C.B.

Supporting Information Available: An image of wetted particle samples, the calculation of main characteristics of C18-derivatized silica particles, and the calculation of particle density for all Models. This material is available free of charge via the Internet at http://pubs.acs.org.

Supplemental Materials I. Photograph of the samples with wetted particles in aqueous surfactant solution.

Fig. I.1. Samples with sedimented particles in aqueous surfactant solution.

Supplemental Materials II. Calculation of main characteristics of C18-derivatized silica particles (pore area, pore volume, pore radius)

The values of pore volume, pore radius and surface area were provided by the manufacturer for underivatized material (bare silica). Also available for C18-derivatized particles were the total carbon content and surface coverage of C18. The nominal diameter of underivatized pores is 93 Å, for a total surface area of underivatized material to be 426 m^2/g silica. After C18 modification, the material has a total carbon content of 17.84% and a C18 bonding density of 3.04 μmol C18/m^2.

For underivatized native silica, V_{pore} is estimated from the surface area (A_{pore}) and radius R:

$$V_{pore} = \frac{A_{pore}\, R}{2} \quad \text{(II.1)}$$

where

$$V_{pore} = \pi R^2 H \quad \text{(II.2)}$$

and

$$A_{pore} = 2\pi R H \quad \text{(II.3)}$$

assuming cylindrical pores. By substituting the values for total surface area and pore radius, the total pore volume is 0.99 mL/g silica. This value agrees with the estimated 1.00 mL/g silica from the manufacturer specifications.

We will also utilize the following properties of the C18 bonded phase:

- density: $d_{C18} = 0.79\ g/mL$ [1],
- molecular weight: $MW_{C18} = 311$ [1],
- number of C atoms of bonded phase: $N_C = 20$ [1], and

- effective molecular volume: $MV_{C18} = 494\ Å^3$ [2].

The pore volume for C18-derivatized Luna silica particles was estimated using two methods. The pore radius and surface area for C18-derivatized pore were then calculated.

Method 1: using density of C18

For one gram of the C18-derivatized silica particles, the mass of the C18 layer is:

$$mass_{C18} = \%C\ \frac{MW_{C18}}{12\ N_C} \qquad \text{(II.4)}\ [1]$$

The calculation leads to a value of 0.231 g C18/g C18-silica. By using:

$$V_{C18} = \frac{mass_{C18}}{d_{C18}} \qquad \text{(II.5)}$$

The volume of bonded phase is 0.293 mL C18/g C18-silica. Considering 1 g of C18-silica particles, the mass of silica is given by:

$$m_{silica} = 1 - mass_{C18} \qquad \text{(II.6)}$$

which leads to 0.769 g silica/g C18-silica. We convert the volume of underivatized pore expressed as mL/g silica to mL/g C18-silica:

$$V_{underiv\ pore}\left(\frac{mL}{g\ C18-silica}\right) = V_{underiv\ pore}\left(\frac{mL}{g\ silica}\right)\ m_{silica}\left(\frac{g\ silica}{g\ C18-silica}\right) \qquad \text{(II.7)}$$

The numerical calculation gives a volume of underivatized pores of 0.761 mL/g C18-silica. Finally, the pore volume of the C18-derivatized silica is:

$$V_{deriv\ pore} = V_{underiv\ pore} - V_{C18} \qquad \text{(II.8)}$$

or 0.469 mL/g C18-silica.

Method 2: using surface coverage and molecular volume of C18

The volume of bonded phase with respect to the fraction of silica in C18-silica is estimated by:

$$V_{C18} = surface\ coverage \cdot surface\ area \cdot Avogadro's\ number \cdot C18\ molecular\ volume \quad \text{(II.9)}$$

The calculation leads to 0.385 mL C18/g silica.

Similar to method 1 (eq. II.6), we use the mass of silica m_{silica} = *0.769 g silica/g C18-silica* to convert the volume of C18 expressed as mL/g silica to mL/g C18-silica:

$$V_{C18}\left(\frac{mL}{g\ C18-silica}\right) = V_{C18}\left(\frac{mL}{g\ silica}\right) m_{silica}\left(\frac{g}{g\ C18-silica}\right) \quad \text{(II.10)}$$

which leads to 0.296 mL C18/g C18-silica.

Finally, the volume of derivatized pore expressed as mL/g C18-silica is:

$$V_{deriv\ pore} = V_{underiv\ pore} - V_{C18} \quad \text{(II.11)}$$

or 0.465 mL C18/g C18-silica.

The pore volume used in this paper for all the calculations represents the average value of methods 1 and 2:

$$V_{deriv\ pore} = 0.467\ \frac{mL}{g\ C18-silica} = 0.47\ \frac{mL}{g\ C18-silica} \quad \text{(II.12)}$$

The radius of derivatized pore is calculated by using the volume of derivatized pore and the volume and radius of pore prior to derivatization:

$$V_{underiv\ pore} = \pi R^2_{underiv\ pore} H_{underiv\ pore} \quad \text{(II.13)}$$

$$V_{deriv\ pore} = \pi R^2_{deriv\ pore} H_{deriv\ pore} \quad \text{(II.14)}$$

$$R_{deriv\ pore} = R_{underiv\ pore}\sqrt{\frac{V_{deriv\ pore}}{V_{underiv\ pore}}} \quad \text{(II.15)}$$

By substituting the values for parameters above, $R_{underiv\ pore} = 46.5\ Å$, $V_{underiv\ pore} = 0.76\ mL/g\ C18\text{-}silica$ and $V_{deriv\ pore} = 0.47\ mL/g\ C18\text{-}silica$, a radius of 36.5 Å is obtained for the derivatized pore.

Finally, the surface area is calculated by using the volume and the radius of the derivatized pore:

$$S_{deriv\ pore} = \frac{2\,V_{deriv\ pore}}{R_{deriv\ pore}} \qquad \text{(II.16)}$$

The value calculated is 256 m^2/g C18-silica.

Supplemental Materials III. Calculation of particle density for Models I, II and III

1. General formula for particle density calculation

The total volume of the particles, V_{total}, is the sum of the C18-silica particles volume V_{solid} (including volumes of both the silica and the C18 layer) and the pore volume V_{pores}, which is occupied by air (V_{air}), adsorbed SDS ($V_{SDS\ adsorbed}$) and the wetting solution ($V_{solution}$):

$$V_{total} = V_{solid} + V_{pores} = V_{solid} + V_{air} + V_{solution} + V_{SDS\ adsorbed} \quad \text{(III.1)}$$

The volumes are calculated with the respective masses (m) and densities (ρ):

$$\frac{m_{total}}{\rho_{total}} = \frac{m_{solid}}{\rho_{solid}} + V_{pores} \quad \text{(III.2)}$$

Sum of the masses gives:

$$\frac{m_{solid} + m_{air} + m_{solution} + m_{SDS\ adsorbed}}{\rho_{total}} = \frac{m_{solid}}{\rho_{solid}} + V_{pores} \quad \text{(III.3)}$$

The mass of adsorbed SDS is determined by its number of moles ($n_{SDS\ adsorbed}$):

$$\frac{m_{solid} + \rho_{solution}\ V_{solution} + n_{SDS\ adsorbed}\ MW_{SDS}}{\rho_{total}} = \frac{m_{solid}}{\rho_{solid}} + V_{pores} \quad \text{(III.4)}$$

The density of a particle modified by SDS and wetting solution is thus:

$$\rho_{total} = \frac{m_{solid} + \rho_{solution}\ V_{solution} + n_{SDS\ adsorbed}\ MW_{SDS}}{\frac{m_{solid}}{\rho_{solid}} + V_{pores}} \quad \text{(III.5)}$$

m_{air} was neglected because its contribution to the total mass is negligible. For example, for completely dry particles ($V_{air} = V_{pores}$), the mass of air is 0.000561 g per g C18-silica when air density is taken for 20°C and 1 bar (0.001194 g/mL [3]). This means that the percentage contribution of air is < 0.0561% for particles modified by SDS and the wetting solution.

The density of C18-derivatized silica particles, ρ_{solid}, was calculated as:

$$\rho_{solid} = \frac{m_{solid}}{V_{solid}} = \frac{m_{silica} + m_{C18}}{V_{silica} + V_{C18}} = \frac{m_{silica} + m_{C18}}{\frac{m_{silica}}{\rho_{silica}} + \frac{m_{C18}}{\rho_{C18}}} = \frac{1}{\frac{w_{silica}}{\rho_{silica}} + \frac{w_{C18}}{\rho_{C18}}} \quad \text{(III.6)}$$

We used m_{solid} = *1 g C18-silica particles* and $m_{silica} = w_{silica}\, m_{solid} = w_{silica}$, $m_{C18} = w_{C18}\, m_{solid} = w_{C18}$, where w_{silica} and w_{C18} represent the mass fractions of silica and C18, respectively, in C18-silica particles. In the particles under study, $w_{silica} = 0.769$, $w_{C18} = 0.231$, $\rho_{silica} = 2.15\ g/mL$ and $\rho_{C18} = 0.79\ g/mL$. We thus have $\rho_{solid} = 1.54\ g/mL$.

The number of moles of adsorbed SDS is:

$$n_{SDS\ adsorbed} = n_{SDS\ adsorbed\ specific} \cdot specific\ surface \cdot m_{solid}$$

where $n_{SDS\ adsorbed\ specific}$ is in mol/m^2, specific surface in m^2/g and m_{solid} in g.

The value of $n_{SDS\ adsorbed\ specific}$, 4.2 x 10^{-6} mol/m^2, is the maximum surface coverage of SDS molecules on the mesoporous silica.

2. Calculation of volumes of all the components inside nanopores in the particle – solution system

The possible components that occupy the nanopores at any moment in time during the adsorption process are: solution, SDS layer adsorbed on the inner wall of nanopores and air.

2a. ***Model I****: SDS molecules adsorb as a compact monolayer vertically oriented on the C18 phase of the nanopores.*

The SDS coverage is defined with respect to the maximum achievable coverage of a compact SDS monolayer:

$$f = \frac{a}{A} \qquad \text{(III.7)}$$

where a is the effective area covered by adsorbed SDS molecules and A the maximum area that can be covered by adsorbed SDS molecules (pore area).

The pore is considered to be a cylinder with a radius equal to the average radius of C18-derivatized silica particles (see Section II for calculation).

$$a = 2\pi\, R\, h \tag{III.8}$$

$$A = 2\pi\, R\, H \tag{III.9}$$

where *R* is the radius of the cylinder, *h* the actual height of the fraction of cylinder that is covered by the adsorbed SDS layer and thus filled by the solution, *H* the total height of the cylinder (nanopores) (Fig. III.1).

Thus:

$$f = \frac{h}{H} \tag{III.10}$$

and

$$V_{pore} = \pi R^2\, H \tag{III.11}$$

$$V_{solution} = \pi r^2\, h = \pi r^2\, f\, H \tag{III.12}$$

$$V_{SDS\ max\ coverage} = \pi R^2\, H - \pi r^2\, H = \pi(R^2 - r^2)H \tag{III.13}$$

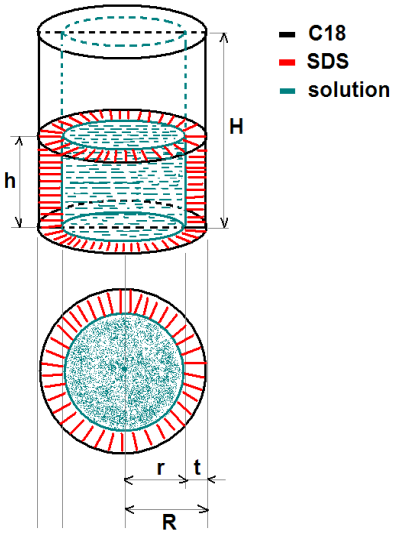

Figure III.1. SDS adsorption as a compact monolayer oriented vertically to surface, guiding solution into the nanopore - ***Model I***.

The volume of the wetting solution is determined by the pore volume and the volume of SDS at the maximum coverage:

$$V_{solution} = f\left(V_{pore} - V_{SDS\,\max coverage}\right) \quad \text{(III.14)}$$

$V_{SDS\ max\ coverage}$ is a function of the pore radius, pore volume and the thickness ***t*** of the SDS adsorbed layer:

$$V_{SDS\,max\,coverage} = \pi(R^2 - r^2)\,H = \pi(R-r)(R+r)\,H = \pi t(2R-t)\frac{V_{pore}}{\pi R^2} = \frac{t(2R-t)}{R^2}\,V_{pore} \quad \text{(III.15)}$$

The volumes of the other two components of the nanopore, adsorbed SDS and air above solution, are:

$$V_{SDS} = f\,V_{SDS\,\max coverage} \quad \text{(III.16)}$$

and

$$V_{air} = V_{pore} - V_{solution} - V_{SDS} \quad \text{(III.17)}$$

With these formulas, the volumes can be simulated for each SDS coverage *f*.

2b. ***Model II***: *SDS molecules adsorb as dispersed individual molecules oriented vertically on the C18 phase of the nanopores; intermolecular space between adsorbed SDS molecules is filled with water.*

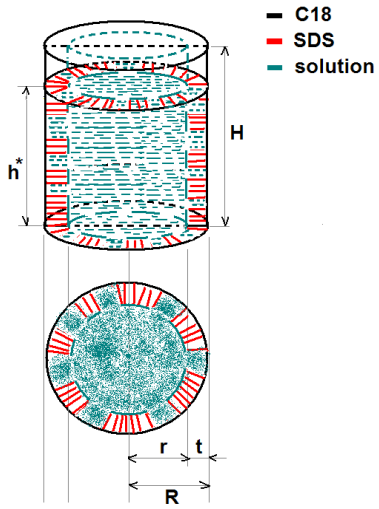

Figure III.2. SDS adsorption as dispersed individual molecules oriented away from surface inducing pore wetting by solution - ***Model II***.

The level of solution into the nanopore can be expressed as:

$$h^* = f^* h = f^* f H \qquad \text{(III.18)}$$

where f is the SDS coverage as defined in Model I and f^* is denoted as the "dispersion factor" and reflects the decrease of charge density on the nanopore surface ($f^* = 1$ means no dispersion and maximum charge density).

The solution will occupy the volume:

$$V_{solution} = V_{solution\ in\ the\ cylinder} + V_{interstitial\ space\ between\ adsorbed\ SDS\ molecules} =$$

$$f^* f \left(V_{pore} - V_{SDS\,\max coverage}\right) + f\,(f^* - 1) V_{SDS\,\max coverage} =$$

$$f\,(f^* V_{pore} - V_{SDS\,\max coverage}) \qquad \text{(III.19)}$$

V_{SDS} and V_{air} are calculated using identical formulas as in Model I.

As a general comment for both Models I and II: although the maximum length of expanded C12 tail of SDS, 16.7 Å (based on Tanford formula[4]), is taken into account it is possible that, for a SDS thickness of 11 Å, a fragment of SDS tail penetrates and intercalates into the C18 layer. This situation is favorable in Model II in order to minimize the direct contact of individual unprotected hydrophobic tails with water.

2c. ***Model III***: *SDS molecules adsorb as dispersed hemisphere-shaped hemimicelles on C18 monolayer; inter-micellar area is wetted with water.*

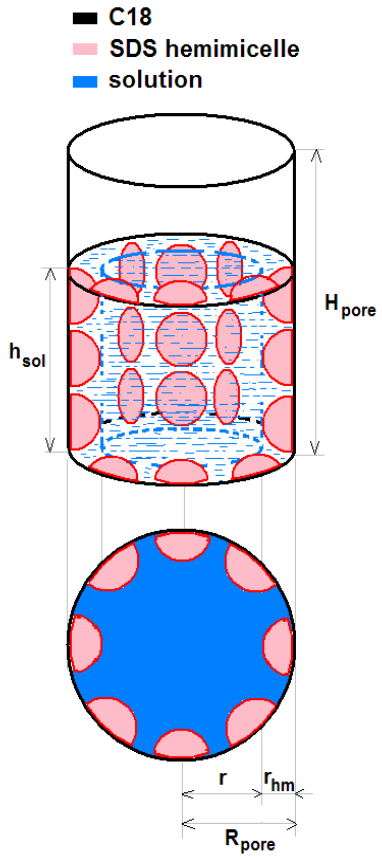

Figure III.3. SDS adsorption as hemispherical hemicelles into nanopore, inducing pore wetting by solution – ***Model III***.

Again, this model considers the pore as a cylinder with radius equal to average radius of C18-derivatized silica particles (Section I). The dispersion factor *f** is defined as the ratio of apparent and effective area of nanopore covered by SDS hemimicelles:

$$f^* = \frac{A_{app\ SDS\ ads}}{A_{eff\ SDS\ ads}} \quad \text{(III.20)}$$

where $A_{app\ SDS\ ads} = 2\pi R_{pore}\, h_{solution}$ (III.21)

$$A_{eff\ SDS\ ads} = No_{hm}\, x\, \pi r_{hm}^2 \quad \text{(III.22)}$$

and No_{hm} is the total number of hemimicelles and is estimated as:

$$No_{hm} = \frac{n_{SDS\ ads}\ \ A_{pore}\ \ N_A}{N_{hm}} \quad \text{(III.23)}$$

where N_{hm} is the aggregation number for the hemimicelle, $n_{SDS\ ads}$ the moles of SDS adsorbed per unit surface, A_{pore} the total pore area and N_A the Avogadro's number.

The volume of solution that rises into nanopore during the wetting process is estimated as:

$$V_{solution} = \pi R_{pore}^2\, h_{solution} - V_{SDS\ ads\ hm} = \frac{V_{pore}}{H_{pore}}\, h_{solution} - V_{SDS\ ads\ hm} \quad \text{(III.24)}$$

$V_{SDS\ ads\ hm}$, the volume of SDS adsorbed that contributes to the volume of hemimicelles, is the sum of the volumes of hydrophobic cores and anionic heads. The volume of the hydrophobic core is determined by the actual number of C atoms that participate in hemimicelle formation (see subsection 3). This number is calculated as the difference between the total number of C (12 in case of SDS) and the number of C atoms of hydrophobic tails that intercalate into the C18 layer:

$$V_{SDS\ ads\ hm} = No_{hm}\, V_{core\ hm} + No_{hm}\, N_{hm}\, V_{head} = No_{hm}\, (V_{core\ hm} + N_{hm}\, V_{head}) \quad \text{(III.25)}$$

in which V_{head} is the volume of SDS head group.

Because $A_{pore} = 2\pi R_{pore}\, H_{pore}$, $\frac{h_{solution}}{H_{pore}} = \frac{A_{app\ SDS\ ads}}{A_{pore}}$ (III.26)

Finally:

$$V_{solution} = \frac{A_{app\ SDS\ ads}}{A_{pore}}\, V_{pore} - V_{SDS\ ads\ hm} = f^* \frac{A_{eff\ SDS\ ads}}{A_{pore}}\, V_{pore} - V_{SDS\ ads\ hm} \quad \text{(III.27)}$$

$$V_{air} = V_{pore} - V_{SDS\ ads} - V_{solution} \quad \text{(III.28)}$$

3. Calculation of hemimicellar radius

The SDS hemimicelle is considered as a hemisphere with two components: an inner hydrophobic core formed by the hydrophobic tails and a charged shell formed by the anionic sulfate groups (Fig. 5). The hydrophobic core is assumed to be impenetrable to solvent molecules or ions (no holes). This assumption is a reasonable one for the simulation although the solvent molecules do penetrate into the core, especially into the outer-most fraction of the hydrocarbon chains. The number of solvent molecules in the core is low and can be neglected in the volume calculation. On the contrary, depending on the aggregation number and the number of C atoms that participate in the hemimicelle formation, water molecules and counterions can penetrate the charged shell and occupy the space between the sulfate groups.

According to Tanford[4], an alkyl chain will occupy a certain volume in the hydrophobic core:

$$v_{chain} = 27.4 + 26.9\, n_C \ \ (in\ \text{Å}^3) \quad \text{(III.29)}$$

As a result, the volume of hemimicelle core becomes:

$$V_{core\ hm} = v_{chain}\, N_{hm} = (27.4 + 26.9\, n_C) N_{hm} \ \ (in\ \text{Å}^3) \quad \text{(III.30)}$$

Because hemimicelle is a hemispehere, the volume of hemimicelle core is also:

$$V_{core\ hm} = \frac{2}{3}\, \pi r_{core\ hm}^3 \quad \text{(III.31)}$$

The radius of the hemimicelle core is a function of its aggregation number and the number of C atoms participating in the hemimicelle formation:

$$r_{core\ hm} = \sqrt[3]{\frac{3N_{hm}\,(27.4+26.9\,n_C)}{2\pi}}\ \ (in\ \text{Å}) \qquad \text{(III.32)}$$

Finally, the hemimicelle radius represents the sum of radius of hemimicelle core and diameter of anionic head group:

$$r_{hm} = r_{core\ hm} + d_{SDS\ head} \qquad \text{(III.33)}$$

The diameter of sulfate group is estimated based on Bruce *et al* [5]. Specifically, the radius of SDS head can be considered as the distance from S atom to the neighbor water O minus the radius of water:

$$d_{SDS\ head} = 2\,r_{SDS\ head} = 2\left(l_{S-O} - r_{H_2O}\right) \qquad \text{(III.34)}$$

The values 3.8 Å for distance between S and O and 1.4 Å for radius of water molecule lead to a diameter of 4.8 Å for SDS head.

Supplemental Materials IV. Calculation of particle density for Model III when formation of a vapor film between water and the wall of hydrophobic nanopore is assumed.

The particle density is calculated in the same way as in the previous section (eq. III.5). The mass of the gas-like fluid that separates water from the hydrophobic wall is neglected due to its insignificant contribution comparing to the other terms in the equation (similar to neglecting mass of air due to its contribution to the total mass). The overall particle density will decrease comparing to no-vapor film situation because of the smaller volume of solution that rises into nanopore during the wetting process. Thus, the volume of the vapor film V_{gp} is subtracted from the term $V_{solution}$ (calculated as in eq. III.27). V_{gp} is estimated as:

$$V_{gp} = (f^* - 1)A_{eff\ SDS\ ads}\ t_{gp} \qquad \text{(IV.1)}$$

where t_{gp} represent the average thickness of the vapor film between water and the wall of hydrophobic nanopore (Figure IV.1).

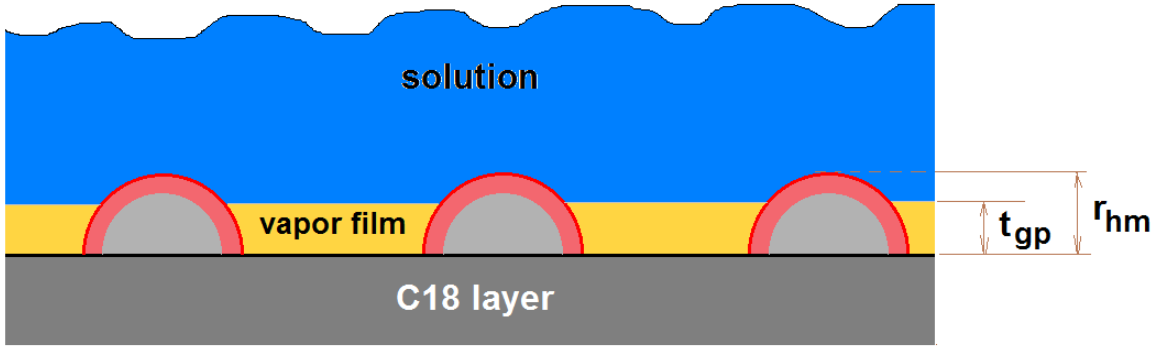

Fig. IV.1. Formation of a vapor film between water (non-wetting liquid) and the C18 layer (hydrophobic surface) in the inter-hemimicelle area.

r_{hm} – hemimicelle radius; t_{gp} – thickness of the vapor film

We calculated the extent of particle density decrease for several types of SDS hemimicelles. We chose two representative combinations ***aggregation number – number of C atoms intercalated into C18 layer*** out of the hemimicelles that obey the steric constraint in Fig. 7B (hemimicelle radius < 11.7 Å). Thus, we selected the hemimicelle with aggregation number 7 and ten C atoms intercalated into C18 layer, denoted as hemimicelle *"7-10"* and the hemimicelle with aggregation number 4 and seven C atoms intercalated into C18 layer, denoted as hemimicelle *"4-7"*. The hemimicelle "7-10" represents one of the structures with a charge density close to the bulk SDS micelles in solution, whereas the combination "4-7" corresponds to hemimicelles with lower charge density. We used 5.6 Å as the thickness of the vapor film. [6]

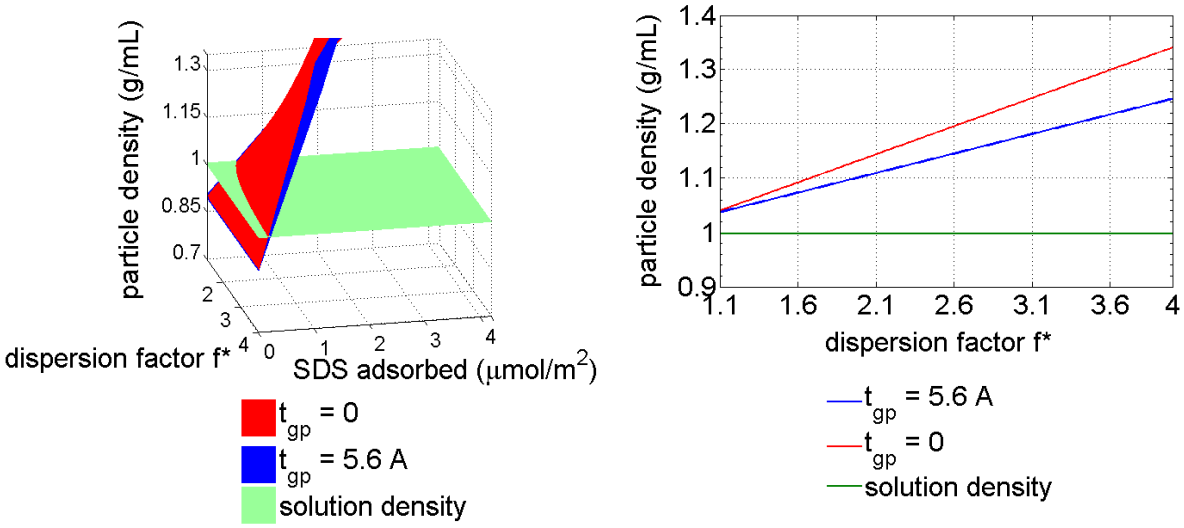

Fig. IV.2. A - Particle density as a function of the amount of SDS adsorbed and dispersion factor *f** for adsorbed hemimicelles with aggregation number 7 and ten C atoms of the SDS tails intercalating into the C18 layer; B - particle density along the entire range of dispersion factor *f** for SDS coverage 0.73 μmol/m^2.

Figure IV.2.A shows comparatively the particle density as function of the dispersion factor f* and SDS coverage for both situations, namely no-vapor film model versus the formation of the vapor film, when hemimicelles "7-10" are formed on nanopores wall. Figure IV.2.B presents the 2D cross-sections through the particle density surfaces at experimental coverage 0.73 μmol/m^2.

Similarly, the cross-sections through the particle density surfaces at experimental coverage 0.73 μmol/m^2 corresponding to formation of hemimicelles "4-7" is shown in fig. IV.3.

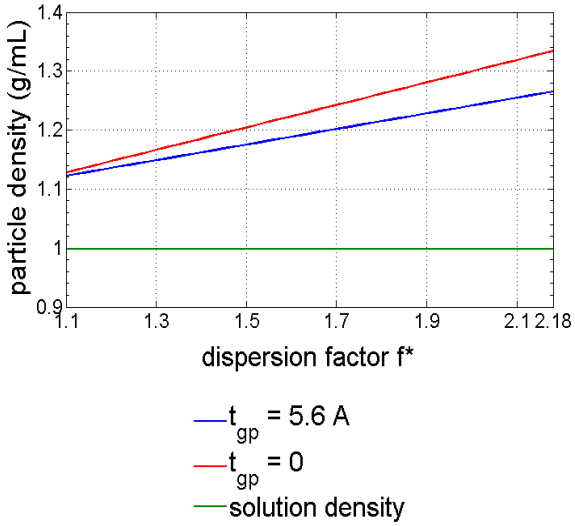

Fig. IV.3. Particle density along the entire range of dispersion factor *f** for the experimental SDS coverage 0.73 μmol/m^2 when SDS adsorbs as hemimicelles with aggregation number 4 and seven C atoms of the SDS tails intercalating into the C18 layer.

Table IV.1 shows the decrease in the overall density of the particles with nanopores completely filled (maximum dispersion factor f*) and SDS coverage of 0.73 μmol/m^2 when the formation of a 5.6 Å vapor film is assumed.

Table IV.1. The decrease in particle density when the formation of a 5.6 Å vapor film between water and nanopore's wall is assumed.

Type hemimicelle	**Thickness vapor film (Å)**	**particle density (g/mL)**	**Dispersion factor f***	**Volume solution (mL/g part.)**	**Volume SDS adsorbed (mL/g part.)**	**Volume vapor film (mL/g part.)**
"7-10"	0	1.341	4	0.450	0.015	0
	5.6	1.246		0.343		0.106
		density decrease (%)		**volume decrease (%)**		
		7.1		23.7		
Type hemimicelle	**Thickness vapor film (Å)**	**particle density (g/mL)**	**Dispersion factor f***	**Volume solution (mL/g part.)**	**Volume SDS adsorbed (mL/g part.)**	**Volume vapor film (mL/g part.)**
"4-7"	0	1.334	2.18	0.442	0.024	0
	5.6	1.265		0.365		0.077
		density decrease (%)		**volume decrease (%)**		
		5.1		17.4		

References

(1) Gritti, F.; Guiochon, G. *Journal of Chromatography A* **2007**, *1176*, 107.

(2) Rustamov, I.; Farcas, T.; Ahmed, F.; Chan, F.; LoBrutto, R.; McNair, H. M.; Kazakevich, Y. V. *Journal of Chromatography A* **2001**, *913*, 49.

(3) ***CRC Handbook of Chemistry and Physics*** 89th ed.; Lide, D. R., Ed., 2008-2009.

(4) Tanford, C. *Journal of Physical Chemistry* **1972**, *76*, 3020.

(5) Bruce, C. D.; Berkowitz, M. L.; Perera, L.; Forbes, M. D. E. *Journal of Physical Chemistry B* **2002**, *106*, 3788.

(6) Helmy, R.; Kazakevich, Y.; Ni, C. Y.; Fadeev, A. Y. *Journal of the American Chemical Society* **2005**, *127*, 12446.